Global and Planetary Change 77 (2011) 49–61

Contents lists available at ScienceDirect

Global and Planetary Change

journal homepage: www.elsevier.com/locate/gloplacha

Two-dimensional reconstruction of the Mediterranean sea level over 1970–2006 from tide gage data and regional ocean circulation model outputs

B. Meyssignac [a,*], F.M. Calafat [b], S. Somot [c], V. Rupolo [d], P. Stocchi [e], W. Llovel [a], A. Cazenave [a]

[a] LEGOS/CNES, 14, Avenue E. Belin, 31400 Toulouse, France
[b] IMEDEA (CSIC-UIB), Miquel Marques, 21, Esporles 07190, Mallorca, Baleares, Spain
[c] Météo-France/CNRS, CNRM-GAME, 31057 Toulouse cedex, France
[d] ACS-CLIM MOD, ENEA, Bldg F19, Room 112 Sp. 91 CR Casaccia, Via Anguillarese 301, 00060 Santa Maria di Galeria, Rome, Italy
[e] DEOS, Faculty of Aerospace Engineering, TUDelft, Delft, The Netherlands

ARTICLE INFO

Article history:
Received 19 January 2011
Accepted 22 March 2011
Available online 29 March 2011

Keywords:
sea level
Mediterranean Sea
reconstruction
interannual sea level variability
altimetry
tide gages
empirical orthogonal functions
Eastern Mediterranean Transient

ABSTRACT

Two-dimensional reconstructions of the Mediterranean sea level corrected for the atmospheric effects are proposed at monthly interval over the period 1970–2006 using 14 tide gage records and 33-year long (1970–2002) sea level grids from the NEMOMED8 regional ocean circulation model (NM8) and the PROTHEUS System Atmosphere–Ocean coupled model (PS). They are compared with a similar reconstruction using decade-long sea level grids from altimetry (Topex/Poseidon and Jason1) and a published reconstruction by Calafat and Gomis (2009). Tests with extra tide gages, not used in the computation, show that interannual variability is better captured when using long (33-year) spatial grids. In particular the NM8-based reconstruction reproduces better the sea level variability at all independent tide gages. An empirical Orthogonal Function decomposition of this reconstruction over 1970–2006 shows that the temporal curve of the two first modes are highly correlated with the North Atlantic Oscillation. We note in particular different behaviors over the 1970–1994 and 1994–2006 time spans. Results suggest that the North Atlantic Oscillation forcing modified the spatial patterns of the Mediterranean sea level around the year 1993 close to the date of occurrence of the Eastern Mediterranean Transient (a major change in the deep water formation of the Levantine and Ionian basin that occurred in the early 1990s).

1. Introduction

Long term sea level rise is a critical issue of the global climate change because of its potential huge impacts (IPCC 2007). It has been extensively studied in recent years in order to understand the driving mechanisms of its spatial and temporal variability. Since 1993, sea level is accurately monitored by satellite altimetry (i.e. Topex/Poseidon, Jason1, Jason2 and Envisat among others) with a global coverage and a short revisit time. These observations have shown that sea level does not rise uniformly. In some regions it rises faster than the global average while in others, the rise is slower (Bindoff et al., 2007). Cabanes et al. (2001), and then Lombard et al. (2005) showed that most of these regional variations could be explained by the geographical variations of ocean thermal expansion although some other processes may also play a role in regional sea level trends (e.g. the solid Earth response to the last deglaciation, Milne et al., 2009). A number of studies have shown that spatial trend patterns in thermal expansion are not stationary but fluctuate in space and time in response to forcing modes of the coupled Atmosphere–Ocean system, such as ENSO (El Nino-Southern Oscillation), PDO (Pacific Decadal Oscillation), NAO (North Atlantic Oscillation) and others (Lombard et al., 2005; Bindoff et al., 2007). Thus the regional variability seen by satellite altimetry over 1993–2009 is likely not representative of the past few decades.

However it is important to know past regional variability and understand how it changes with time on interannual/decadal/multi-decadal time scales. This helps to understand the local dominant modes of variability and assess the potential regional impacts of sea level rise. It is particularly important in vulnerable populated area such as the Mediterranean basin. Unfortunately, for the past decades, there are no direct basin-scale observations informing on spatial trend patterns in Mediterranean sea level. In this study, we develop a reconstruction method of past Mediterranean sea level (since 1970) that combines long tide gage records of limited spatial coverage with 2-D sea level patterns based either on satellite altimetry or on runs from Regional Ocean circulation Models (here after noted ROM) (see Section 2 below for the description of the models). Gridded time series that cover the whole Mediterranean basin over the tide gage records time span are obtained as a result, giving some information on the past spatial trend patterns variability in Mediterranean sea level.

* Corresponding author at: LEGOS, 14 Avenue Edouard Belin, 31400 Toulouse, France. Tel.: +33 5 61 33 29 90; fax: +33 5 61 25 32 05.
E-mail address: benoit.meyssignac@legos.obs-mip.fr (B. Meyssignac).

0921-8181/$ – see front matter © 2011 Elsevier B.V. All rights reserved.
doi:10.1016/j.gloplacha.2011.03.002

Such a reconstruction method has previously been developed for the global sea level over the past 50 years by Church et al. (2004) and Llovel et al. (2009). For the Mediterranean sea, a regional reconstruction is also available from Calafat and Gomis (2009) (hereafter C&G). They used the optimal interpolation method of Kaplan et al. (2000) (as used in Church et al., 2004) to interpolate the long tide gage records with the spatial patterns of the 2-D sea level grids from altimetry. In this study we expand the earlier work of C&G by reconstructing with the same method, the atmospheric-corrected Mediterranean sea level variability. Indeed, C&G did not correct the sea level data for the inverted barometer – IB – effect (the response of the sea surface to atmospheric pressure). In the Mediterranean sea, this signal is strong (Tsimplis and Josey (2001), Marcos and Tsimplis (2007)). If one is interested in the climate variability signal only, it should be removed. By making use of atmospheric-corrected Mediterranean sea level we get a closer view of the long-term, non-meteorological influence on the Mediterranean sea level. The study by C&G used as well spatial patterns (spatial component of the EOFs of the sea level, see Section 2) deduced from satellite altimetry over a limited time span (13 years: 1993–2006), a period affected by the strong change in the central and eastern Mediterranean circulation that occurred in the early 1990s: the Eastern Mediterranean Transient (EMT hereafter) (Roether et al., 1996; Klein et al., 1999; Lascaratos et al., 1999; Theocharis et al., 1999; Zervakis et al., 2004; Roether et al., 2007). The EMT is characterized by a change in the Eastern Mediterranean deep water characteristics. For almost the entire 20th century, these deep waters were of Adriatic origin, and in the early 1990s they were formed in the Aegean Sea after some climatic events; among them, a change in the surface circulation of the Ionian and Levantine basin (Malanotte-Rizzoli et al., 1999; Samuel et al., 1999; Theocharis and Kontoyiannis, 1999), an intense winter convection in the Aegean Sea in 1987 and two successive very cold winters in the Aegean Sea in 1992 and 1993 (Josey, 2003; Beuvier et al., 2010). The EMT impacted the Mediterranean circulation during the 1990 and still has an influence nowadays (Roether et al., 2007). It seems to be responsible for a change of surface circulation from anti-cyclonic to cyclonic in the Ionian basin in 1998 (Tsimplis et al., 2009; Vera et al., 2009) and may have interannual to interdecadal impacts on sea level variability as suggested by Tsimplis et al. (2005). In particular the EMT is likely to have strongly impacted the Mediterranean sea level patterns over the short altimetry period, making them exceptional and poorly representative of the past decades patterns. This non-stationarity of the sea level patterns in time and space can alter the reconstruction of the past sea level (see Llovel et al., 2009). By making use of short term sea level spatial patterns from altimetry that are dominated by the EMT, C&G reconstruction may be too much influenced by this exceptional event which seems to have occurred once in the XXth century (Beuvier et al., 2010). In this study, in addition to a reconstruction based on short term sea level patterns deduced from altimetry (like in C&G), we develop two other reconstructions on the basis of long-term sea level patterns deduced from models instead of altimetry on the assumption that they better capture the decadal variability of the spatial trend patterns.

The long-term sea level patterns are computed from long runs of ROM of the Mediterranean basin: the ARPERA-forced NEMOMED8 model (Sevault et al., 2009; Beuvier et al., 2010; Herrmann et al., 2010) (NM8 here after) and the coupled model PROTHEUS SYSTEM (Artale et al., 2009) (PS here after). These long-term model outputs (we took 33 years of simulation; between 1970 and 2002 because the PS model ends in 2002, see below) are used with the hope that they provide better representative sea level patterns of the whole reconstructed period 1970–2006 (instead of only the EMT period). The resulting reconstructions are compared to an altimetry-based reconstruction computed with the same tide gage dataset, and with the C&G reconstruction corrected a posteriori for the Inverse Barometer – IB – effects over the common period (i.e. 1970–2000).

The advantage of the approach proposed in this study is twofold: (1) the direct reconstruction of the IB-corrected sea level variability should ensure a reliable reconstruction of the low residual sea level variability only influenced by non-meteorological effect in the Mediterranean region, (2) the 33-year long coverage of the ROM grids in principle minimizes the possible non stationarity of the spatial patterns during the altimetry period (because of the exceptional EMT event).

The structure of the work is as follows. We first select and process the data used to carry out the 3 reconstructions (i.e. the tide gage dataset and the 2-D sea level grids from altimetry and the two ROMs. See Section 2). The methodology of sea level reconstruction is presented in Section 3. In Section 4, the results of the three reconstructions over 1970–2006, in terms of Empirical Orthogonal Functions (EOFs) and maps of spatial trends, are given and validated by comparisons with altimetry and extra tide gage records not used in the reconstruction processes. All results are summarized, discussed and compared in Section 5 before the conclusion.

2. Datasets processing

2.1. Tide gage records

The tide gage records used for the reconstruction were selected among the monthly sea level series available from the database of the Permanent Service for Mean Sea Level (PSMSL) (Woodworth and Player, 2003). The longest continuous records were chosen to get the longest reconstruction. Only 10 records longer than 40 years were available while a minimum of 13 records is needed to get a consistent reconstruction (see Section 4). The best trade-off between longest time span and minimum number of tide gage records made us finally select 13 records from the PSMSL database that span the 36 years period: 1970–2006. All these records are on the north coast of the Mediterranean. To compensate this geographical bias, an extra tide gage record from Alexandria (Egypt) over 1970–2006 was added. The Alexandria record is incomplete in the PSMSL database. However, an updated record was provided to us by O. Frihy of the Coastal Research Institute at Alexandria (Frihy et al., 2010). The tide gage dataset used for the reconstruction had finally 14 records sparsely distributed around the Mediterranean.

The location of the 14 tide gages is shown in Fig. 1 (black dots). All records (except Alexandria) are Revised Local Reference (RLR) data. The RLR label ensures that the records do not contain datum shifts resulting from re-leveling adjustments reported by the PSMSL datum history. In this study the reduction to common reference datum is useless since the reconstruction process uses changes in tide gage sea level instead of absolute tide gage sea level (see Section 3) but jumps in the records would have undoubtly an impact on the decadal reconstructed sea level variability if not corrected. For this reason, the Alexandria record was checked with a shift detector based on the generalized likelihood ratio statistic developed by Becker et al. (2009) to verify that no datum shifts was to be found over the 1970–2006 period. Moreover we checked that the updated Alexandria tide gage record (Frihy et al., 2010) is consistent with the Alexandria record from the PSMSL over the common period 1970–1989. Among the 13 records left, some presented gaps larger than 2 years: Soudhas (Greece), Siros (Greece) and Marseille (France). For the Soudhas that ends in 2002, and the Siros record that has a gap of 13 years between 1984 and 1997, PSMSL provides some extra data called metric record: the term “metric” refers to non-RLR records in the PSMSL database. So we completed them until 2006 with their respective metric record. The RLR records were concatenated with their respective metric record ensuring that the global mean equaled the mean of the long RLR record. The Marseille RLR record only shows a small gap of ~2.5 years between 1996 and 1999. Following the same approach, we completed this gap with the Toulon record since these records show a very high correlation of 0.90 (at a significance level (SL) of more than 99%) over the common time span. For the Venezia (Punta della Salute) record ending in 2000, no metric record was actually available from PSMSL but the Italian tide gage network (www.idromare.it) provides data that covers the period 1986 to 2010. We completed the Venezia RLR

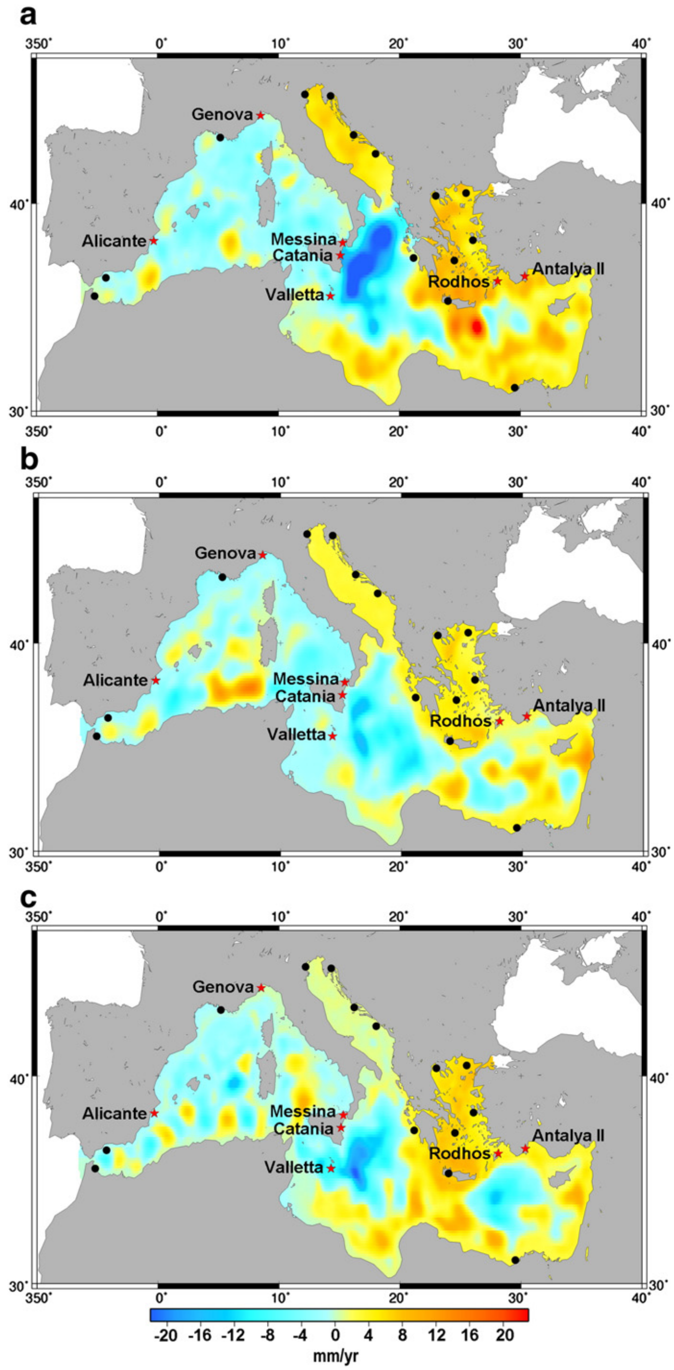

Fig. 1. Trend maps over 1993–2000 from altimetry (a), PS (b) and NM8 (c).

record using data from Idromare website concatenating the two datasets. The Malaga tide gage record span the whole reconstruction period but it shows an unrealistic large trend of 13.9 mm/yr over the period 1993–2010 while the RLR records of its neighbor tide gages present much lower trends, of the order of 6 mm/yr (6.0 mm/yr for Algeciras, 6.6 mm/yr for Tarifa over the same period). The new tide gage situated in Malaga (so called Malaga II in the PSMSL database) shows a similar trend of 6.0 mm/yr. When comparing both tide gages (Malaga and Malaga II), it appears that they fit well over the period 1993.0–1996.5 but beyond the data gap of 1997, the Malaga record drifts upward at a rate of 9.6 mm/yr with respect to the Malaga II record. Assuming that the record of Malaga II is more reliable (its trend over 1993–2010 is consistent with Tarifa and Algeciras) we replaced the record of Malaga by the record of Malaga II over the common period 1993–2010, ensuring that over the period of agreement (1993.0–1996.5) the two records agree. In each of the 14 records, the small gaps that remained (smaller than 2 years) were filled in with a linear interpolation.

To focus on the interannual and decadal time scale of the sea level variability, before filling the gaps and applying the IB correction, we removed from the records the annual and semi annual signal through a harmonic analysis. The analysis was done on the common period 1970–2006 to allow the fitting of a consistent signal in the dataset since the annual cycle is not constant in time (Marcos and Tsimplis, 2007).

The tide gage data were corrected from the static inverted barometer response (IB) of sea level to atmospheric loading using surface pressure fields from the National Centers for Environmental Project (NCEP) (Kalnay et al., 1996).

Tide gages measure sea level relative to the ground, hence also register vertical ground motions. For comparison or combination with altimetry-based sea level data (which are free from ground motions), vertical displacements need to be corrected for. While most tide gage analyses account for the Glacial Isostatic Adjustment (GIA hereafter) whose correction is available from models (Peltier, 2004; Stocchi and Spada, 2009), other contributions such as tectonics, volcanism, sediment load for which little quantitative information is available, are generally neglected. Nevertheless estimates of the total vertical displacements at some tide gage sites have been obtained thanks to GPS techniques (Steigenberger et al., 2006; Woppelmann et al., 2007, 2009). In this study we use land motion estimates by Woppelmann et al. (2009), to correct the tide gages of Marseille, Venezia, Dubrovnik and Ceuta of their vertical displacement. For other tide gages, where these corrections were not available, we only took into account the GIA effect using the model of Stocchi and Spada (2009).

2.2. Satellite altimetry dataset

To estimate the spatial structure of Mediterranean sea level variability, the first option was to use the AVISO satellite altimeter dataset (as in C&G). Weekly high resolution maps of sea level anomalies refined over the Mediterranean Sea were obtained from AVISO (http://www.aviso.oceanobs.com) on a 1/8° regular grid for the 13 year period January 1993–December 2005 (http://www.aviso.oceanobs.com/en/data/products/sea-surface-height-products/regional/m-sla-mediterranean/index.html). We used the DT-MSLA "Ref" series computed at CLS by combining several altimeter missions, namely: Topex/Poseidon, Jasons1 and 2, Envisat and ERS 1 and 2. It is a global homogenous intercalibrated dataset based on global crossover adjustment (Le Traon and Ogor, 1998) using Topex/Poseidon and then Jason1 as reference missions. The Mediterranean DT-MSLA "Ref" series are a subsampled dataset filtered and corrected from the long wavelength error (Le Traon et al., 1998) with specific regional criteria dedicated to the Mediterranean basin. These data are corrected from tides, wet/dry troposphere and ionosphere (see Ablain et al., 2009 for more details). The IB correction has also been applied in order to minimize aliasing effects (Volkov et al., 2007) through the MOG2D barotropic model correction (Carrere and Lyard, 2003) that includes the dynamic ocean response to short-period (<20-day) atmospheric wind and pressure forcing and the static IB correction at periods above 20-day (see Carrere and Lyard, 2003 for details).

We removed the annual and semi annual signal from the dataset through a harmonic analysis over the whole period (January 1993–December 2007). We corrected as well the altimeter-derived sea level from the GIA correction provided by Stocchi and Spada (2009) over the Mediterranean Sea. At this regional scale, the GIA correction value is of the order of −0.24 mm/yr (between −0.26 mm/yr and −0.22 mm/yr).

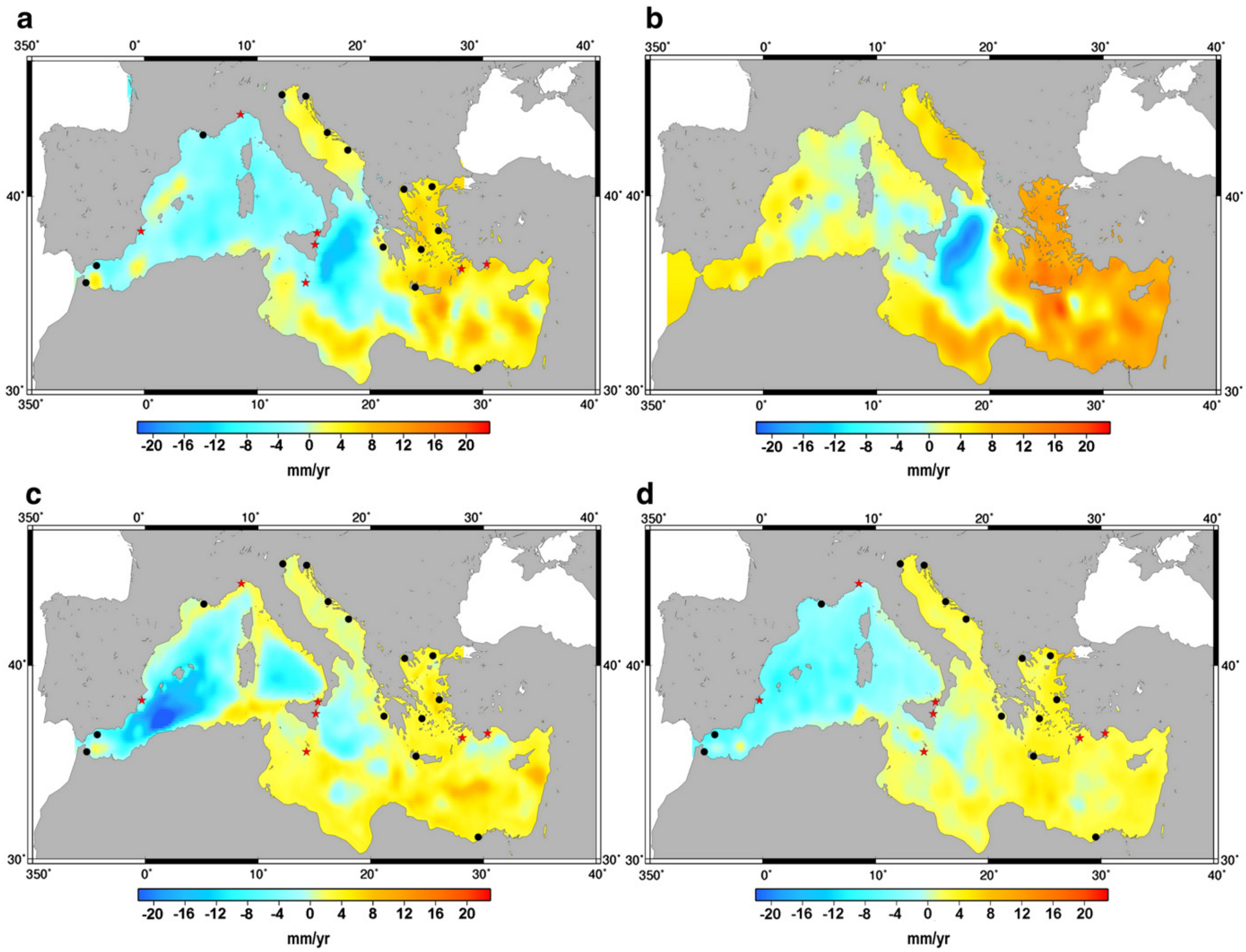

Fig. 2. Trend maps over 1993–2000 from altimetry-based reconstruction (a), Calafat reconstruction (b), PS-based reconstruction (c) and NM8-based reconstruction (d).

2.3. Mediterranean circulation models outputs

As an alternative option to capture the long-term (~20 year periods) spatial structures of Mediterranean sea level variability, we tested the reconstruction with gridded sea level fields obtained from two different ROM simulations: NM8 (Sevault et al., 2009; Beuvier et al., 2010) and PS (Artale et al., 2009).

2.3.1. The NM8 model

The high resolution model NM8 is a Mediterranean configuration of the NEMO ocean model (Madec, 2008). It has an horizontal resolution of $1/8° \times 1/8°$ and a vertical resolution of 43 non-uniform levels (with a resolution varying from 6 m at the surface and 200 m at the bottom). The evolution of the surface of the sea is parametrized by a filtered free-surface (Roullet and Madec, 2000). During the simulation, the volume of the Mediterranean sea is kept constant by redistribution of the evaporated water in the Atlantic buffer zone. The model was used in a simulation over the 1961–2008 period from which we extracted the 33 year period: 1970–2002 (this 33 year simulation will be referred here in after as the NM8 simulation) (Herrmann et al., 2010).

The atmospheric forcing is based on a dynamical downscaling of the ERA40 (Uppala et al., 2005) and of the ECMWF reanalysis filtered at the ERA40 resolution after year 2001. This dynamical downscaling is based on a spectral nudging technique that constrains the large scales (>250 km) of the prognostic variables (air temperature, wind components and logarithm of the surface pressure) to follow the ERA40 chronology and that lets the smaller scales (from 250 km to 50 km) free to develop. The spatial filtering of the ECMWF analysis fields and the non-nudging of the humidity field allow keeping as much as possible a temporal consistency in 2001. The downscaling used in this simulation is named ARPERA (Herrmann and Somot, 2008; Herrmann et al., 2010), it was carried out by the climate model ARPEGE-Climate (Déqué and Piedelievre, 1995). It allows getting high resolution (50 km along the horizontal directions) forcing with a real temporal chronology over the Mediterranean basin. Here the daily mean fields of momentum, fresh water flux (Evaporation minus Precipitations) and net heat flux from ARPERA were used to force NM8 ensuring that NM8 is driven by high resolution air-sea fluxes, homogeneous over the simulation duration (no changes in the ARPEGE configuration between 1970 and 2006) with a realistic interannual variability. The NM8 simulation was forced by climatologic interannual values for the river runoff fluxes, the Black sea inflow and the Atlantic boundary conditions when available or climatologic values otherwise (see Herrmann et al., 2010 for more details). The simulation used here started in August 1960 after a 15-year spin-up under the 1960s atmosphere conditions. The initial conditions were also representative of the 1960s following data from Rixen et al. (2005). Besides a careful overall validation of the NM8 simulation, it has been proved that the NM8 simulation forced by ARPERA air–sea fluxes gives a very realistic representation of the EMT event in the 1990s (Beuvier et al., 2010) and of the Western Mediterranean Deep Water formation (Herrmann et al., 2010). This

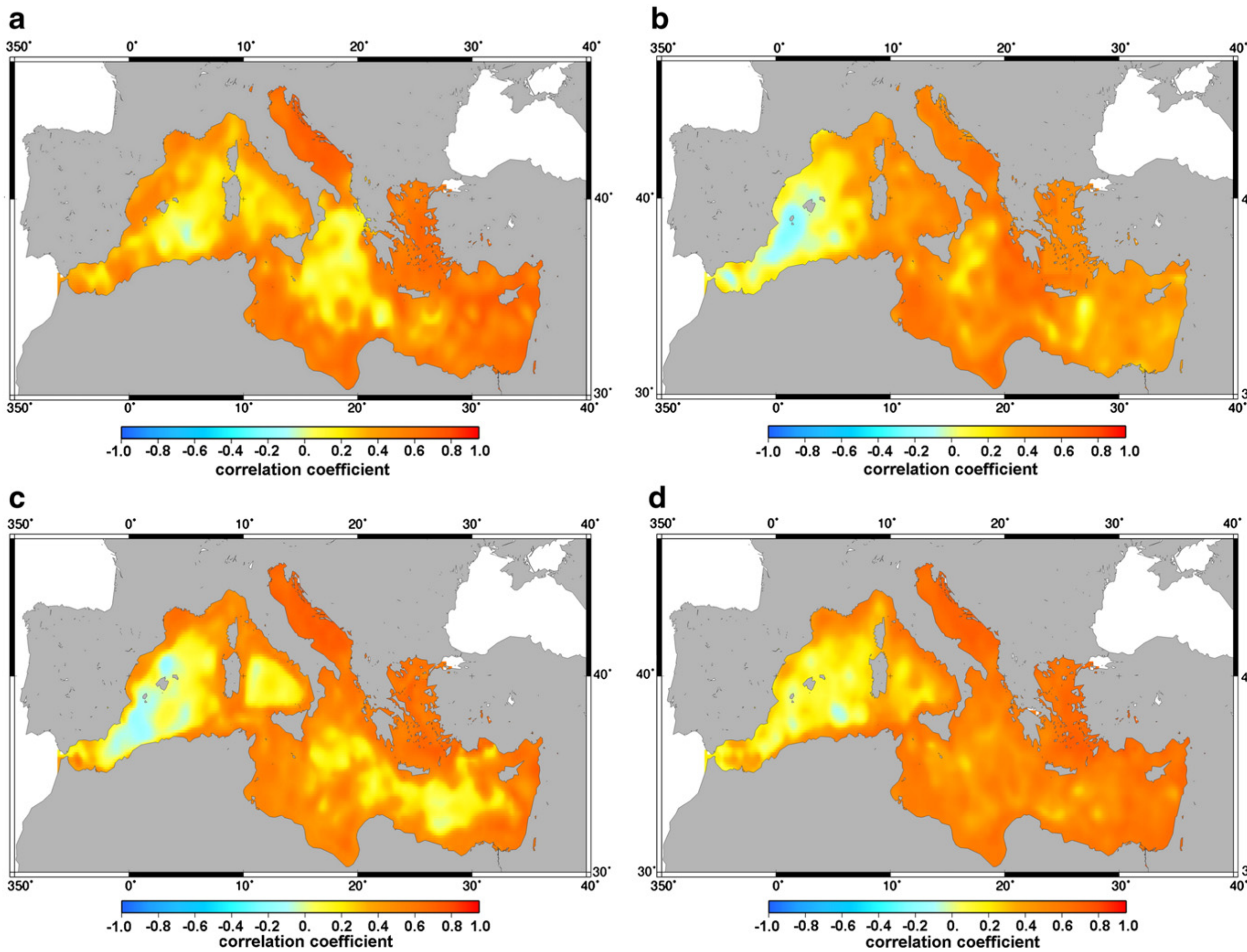

Fig. 3. Correlation maps over 1993–2000 between altimetry and our altimetry-based reconstruction (a), C&G reconstruction (b), PS-based reconstruction (c) and NM8-based reconstruction (d).

version of NM8 includes the coding of the sea level including the absolute steric sea level but excluding the pressure effect and the changes in the Atlantic Ocean sea level.

2.3.2. The PS model

The PS model is an Atmosphere–Ocean regional climate model for the Mediterranean basin. It is composed of the RegCM3 atmospheric regional model (Pal et al., 2007) and a Mediterranean configuration of the MITgcm ocean model (Artale et al., 2009) coupled through the OASIS3 coupler (Valcke and Redler, 2006). In the current study, we only use the outputs of the ocean component of PS that is to say The MITgcm model. It is a free-surface model with $1/8° \times 1/8°$ horizontal resolution and 42 non-uniform vertical levels (with a resolution varying from 10 m at the surface and 300 m at the bottom). The volume of the Mediterranean sea is kept constant during the 37 year simulation as in NM8 but since the freshwater forcing (Evaporation minus Precipitation minus river runoff) is applied as a virtual salt flux, here the net volume transport through the Strait of Gibraltar is zero. Atmospheric forcing (wind stress, heat fluxes, evaporation and precipitation) is computed by the RegCM3 (RegCM3 is a 3-dimensional, sigma coordinate hydrostatic regional climate model with a uniform horizontal resolution of 30 km). Only the river runoff fluxes are climatologic values computed apart (Struglia et al., 2004). The inflow from the Black sea is considered as an extra river flux. In this simulation the lateral boundary conditions are supplied by the ERA40 reanalysis (Uppala et al., 2005) while the MITgcm component provides the Sea Surface Temperature (SST) field.

The PS run starts in 1958 and ends in 2002. For consistent comparisons with the NM8 model, we extracted from this simulation the 33 years period 1970–2002.

From both simulations, total sea level change is computed as the sum of circulation and steric components. The circulation sea level change is given by the surface deformation while the steric sea level change is deduced at each grid point from the vertical integration of the specific volume anomaly caused by temperature and salinity anomalies. When computing global mean sea level from ocean reanalyses, it is classical to apply a basin-averaged, time-varying factor corresponding to the uniform steric effect (as explained by Greatbatch, 1994). However, here this correction is useless because we remove the total basin-average time varying sea level from the models (and the altimetry when it is used). Indeed we only use the spatial patterns of the sea level from the models (or the altimetry) to interpolate the tide gage records and reconstruct the past Mediterranean sea level. Moreover since we are only interested in the interannual to multidecadal sea level fluctuations, the annual and semi annual signals were removed as well from both sea level fields through an harmonic analysis over the whole period January 1970–December 2002.

Fig. 1 shows the trends over 1993–2000 of the sea level computed from a) altimetry, b) the PS run and c) the NM8 run. The very good agreement between the three maps confirms that the two ROM runs reproduce well the Mediterranean sea level at least over the last decade. The signal in the ROM runs appears slightly smaller but the negative patterns of the Western and Ionian basin and the positive pattern of the Aegean basin are consistent with the altimetry.

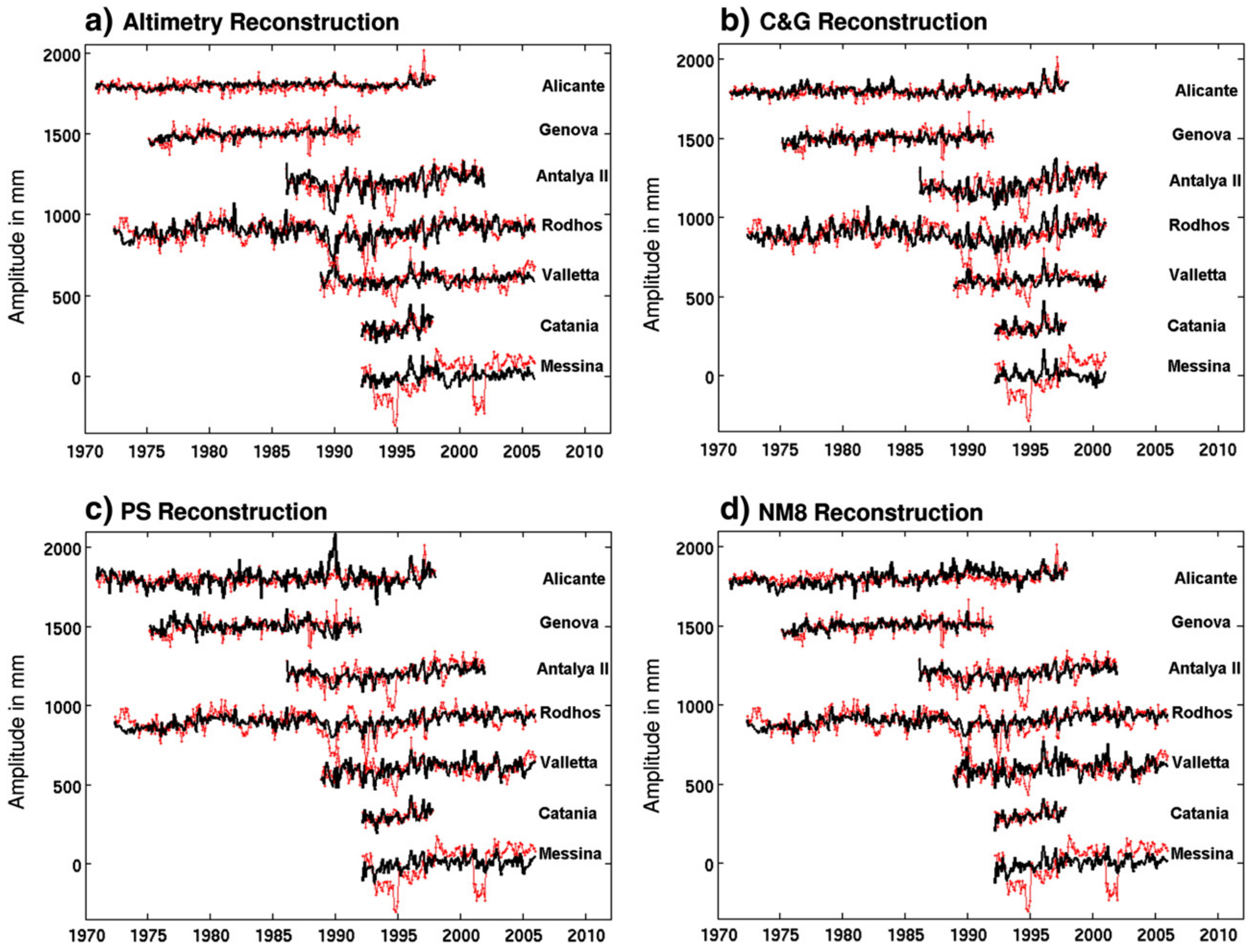

Fig. 4. Comparison of the altimetry reconstruction (a), Calafat reconstruction (b), PS-based reconstruction (c) and NM8-based reconstruction (d) with the tide gages of Alicante, Genova, Antalya II, Rodhos, Valletta, Catania and Messina (from top to bottom on the figure).

3. Reconstruction methodology

The method used to reconstruct past (over 1970–2006) sea level in 2 dimensions over the Mediterranean Basin is based on the reduced optimal interpolation described by Kaplan et al. (2000) and used by Church et al. (2004) and C&G to reconstruct past sea level. The idea consists in interpolating in 2-D the long tide gage records thanks to a time varying linear combination of the spatial patterns of a 2-D sea level grid (either Altimetry or ROMs). This method has 2 steps. In the first step an EOF decomposition (Preisendorfer, 1988; Toumazou and Cretaux, 2001) of a 2-D sea level grid (from altimetry or a Regional Circulation Model) is done. This decomposition allows to separate the spatially well resolved signal (here represented by a matrix H, with m lines for each spatial point and n columns for each date) into spatial modes (EOFs) and their related temporal amplitude as follow:

$$H(x, y, t) = U(x, y)\alpha(t). \quad (1)$$

In this equation $U(x,y)$ stands for the spatial modes and $\alpha(t)$ for their amplitude. Assuming that the spatial modes $U(x,y)$ are stationary in time (see the discussion below), we deduce that the reconstructed sea level field of the Mediterranean basin over the long period 1970–2006 (called here $H_R(x,y,t)$) has an Empirical Orthogonal Decomposition as follow:

$$H_R(x, y, t) = U(x, y)\alpha_R(t)$$

where $\alpha_R(t)$ represents the new amplitudes of the EOFs over 1970–2006.

The second step consists of computing the new amplitudes over the whole period 1970–2006 thanks to the tide gage records. It is done through a least square optimal procedure that minimizes the difference between the reconstructed field and the tide gage records at the tide gage locations.

In the first step, the EOF modes and amplitudes of the 2-D sea level grids are computed through a singular value decomposition approach, such that:

$$H = USV^t \quad (2)$$

where $U(x,y)$ still stands for the EOF spatial modes, S is a diagonal matrix containing the singular values of $H$and Vrepresents the temporal eigen modes. At this stage the amplitude of the EOF modes can be simply written as $\alpha(t) = SV^T$. Conceptually, each EOF k (kth column of $U(x,y)$ multiplied by the kth line of $\alpha(t)$:$U_k(x,y).\alpha_k(t)$) is a spatio-temporal pattern of sea level variability that accounts for a percentage of the total variance of the sea level signal.

The low-order EOFs (eigenvectors of the largest singular values) explain most of the variance and contain the largest spatial scales of the signal. The higher-order EOFs contain smaller spatial scale patterns and are increasingly affected by noise. Besides, their amplitude is decreasingly well resolved by the least squares procedure because the sparseness of the set of in situ gages does not allow resolving too small scale patterns. For efficiency, the reconstruction over the Mediterranean basin uses a subset of the Mlowest-order EOFs (the best fit between maximum variance explained and minimum noise perturbation led us to choose $M = 3$, which account for at least 69% of

Table 1
Correlation and trend's differences between the independent tide gage records (indicated by stars on the maps and shown in Fig. 1) and the corresponding reconstructed time series. Correlations and trend differences are computed over 2 different periods: until 2001 to be able to compare them with the reconstruction of Calafat and Gomis and until 2006 to have the correlations over the whole reconstructed time span. All the correlations computed have a significance level higher than 99% (except for the correlation between the C&G reconstruction and the Messina record).

Name of the tide gage	Calafat and Gomis reconstruction		Altimetry-based reconstruction				PS-based reconstruction				NM8-based reconstruction			
	Corr	Trend	Correlation		Trend difference in mm/yr		Correlation		Trend difference in mm/yr		Correlation		Trend difference in mm/yr	
	→ 2001	diff → 2006	→ 2001	→ 2006	→ 2001	→ 2006	→ 2001	→ 2006	→ 2001	→ 2006	→ 2001	→ 2006	→ 2001	→ 2006
Alicante	0.67	− 0.3 ± 0.4	0.59	0.59	− 0.1 ± 0.4	− 0.1 ± 0.4	0.44	0.44	0.0 ± 0.7	− 0.1 ± 0.7	0.50	0.50	1.9 ± 0.5	1.9 ± 0.5
Genova	0.54	− 1.8 ± 1.0	0.49	0.49	0.2 ± 1.1	0.2 ± 1.1	0.42	0.41	− 3.4 ± 1.1	− 3.4 ± 1.1	0.59	0.59	− 1.1 ± 1.0	− 1.1 ± 1.0
Antalya II	0.48	1.8 ± 2.3	0.43	0.46	− 1.6 ± 2.3	− 2.2 ± 2.1	0.47	0.51	− 2.5 ± 2.0	− 3.0 ± 1.8	0.46	0.50	− 2.6 ± 2.1	− 3.1 ± 1.8
Rodhos	0.39	1.07 ± 0.9	0.57	0.55	0.3 ± 0.7	0.0 ± 0.6	0.55	0.54	1.6 ± 0.7	1.1 ± 0.6	0.56	0.55	1.3 ± 0.7	0.8 ± 0.5
Valletta	0.45	− 2.8 ± 2.1	0.25	0.27	− 3.8 ± 2.5	− 2.1 ± 1.4	0.36	0.40	2.9 ± 2.6	0.2 ± 1.5	0.32	0.39	0.7 ± 2.8	− 0.5 ± 1.6
Catania	0.54	− 6.9 ± 4.9	0.51	0.51	3.2 ± 6.6	3.2 ± 6.6	0.67	0.67	0.2 ± 4.7	0.1 ± 4.7	0.69	0.69	− 0.4 ± 4.2	− 0.4 ± 4.2
Messina	− 0.08	− 27.4 ± 6.6	0.10	0.16	− 23.6 ± 6.8	− 12.4 ± 3.7	0.30	0.28	− 17.5 ± 6.8	− 11.7 ± 3.6	0.31	0.32	− 18.1 ± 6.7	− 11.0 ± 3.6

the total variance of the sea level grid data). Consequently, the data matrix H can be written as:

$$H_M = U_M(x,y).\alpha(t)$$

where $\alpha(t) = S_M V_M^T$ is the matrix of the amplitude of the Mlowest EOFs. Following Kaplan et al. (2000), in the second step, we compute, at each time step over the time span of the in situ records, the amplitudes by minimizing the cost function:

$$S(\alpha) = \left(PU_M\alpha - H^0\right)^T R^{-1}\left(PU_M\alpha - H^0\right) + \alpha^T \Lambda^{-1}\alpha \qquad (3)$$

In $S(\alpha)$, H^0 is the sea level observed by the tide gages, $P$is a projection matrix equal to 1 when and where in situ records are available and 0 otherwise and $\Lambda$is a diagonal matrix of the largest eigenvalues of the covariance matrix. R is the error covariance matrix accounting for the data error covariance matrix (instrumental error) and the error due to the truncation of the set of EOFs to only the first M EOFs. The second term on the right hand side of the function is a constraint on the EOF spectrum of the solution. It prevents the least squares procedure to be contaminated by high-frequency noise (it filters out non significant solutions that display too much variance at grid points without nearby observations). The least squares procedure is then applied to the virtual in situ tide gage records (H^0). It provides the reconstructed amplitude α_R of the EOFs.

Since tide gage records are all relative to their own local datum that are not cross-referenced over the basin, this solution may be polluted by spatial variability of the in situ tide gage records reference surface not necessarily consistent with the altimetry reference surface or the ROM reference surface. To cope with this problem, we have solved Eq. (3) for changes in sea level between adjacent steps following Church et al. (2004). Once changes in amplitude have been obtained at each time step, the amplitudes themselves have been recovered, integrating backward in time. The integration constants are chosen to equal the reconstructed EOF amplitudes mean to the 2-D gridded sea level EOF amplitude mean over the 2-D gridded sea level field period, ensuring consistency between both sets of EOFs.

Another issue with sea level reconstruction in the Mediterranean basin is the strong basin-average signal of the Mediterranean basin. This signal, that is contained in the tide gages, is hardly captured by the few EOFs we use. The reason is that before the computation of the EOFs, for each gridded times series (the 2 ROMs and the altimetry) we have removed the basin-averaged time varying sea level (see Section 2) so the set of EOFs we use is not adapted to reconstruct any basin average sea level. Hence, as in Church et al. (2004), we added in the set of EOFs a spatially uniform EOF (so called EOF0 in Church et al., 2004 and in C&G) to capture, from the tide gages, the basin-averaged signal of the Mediterranean in the past. An advantage of this procedure is that it avoids pouring the strong basin-average sea level signal in different EOFs. Note that tests carried out with and without the EOF0 resulted in almost the same reconstructions.

Finally the reconstructed field of sea level is obtained by multiplying the first three EOFs plus the EOF0 with their reconstructed amplitude:

$$H_R = U_M(x,y)\cdot\alpha_R(t) \qquad (4)$$

At this point, the correction for the atmospheric effects of the tide gage dataset and the altimetry dataset appears particularly important because of the sparsely distribution of the tide gage data set. Indeed, changes over time in atmospheric pressure patterns can be misrepresented with such a sparse network of tide gages biased toward the north of the Mediterranean basin. For example if atmospheric pressure patterns had a bias toward the north in the past this would be misinterpreted as a change in past global Mediterranean sea level although it is not the case. As discussed above, beyond 20-day periods, the correction applied to account for the ocean response to atmospheric forcing is the static IB (1 mbar corresponds to 1 cm sea level). It is known that in the Mediterranean Sea, there is a slight low-frequency non static component. However this effect remains small (a few% of the static part) and for the purpose of the present study can be neglected (F. Lyard, personal communication).

4. Reconstructed sea level

4.1. Validation over the altimetry period

A first way to check the validity of the reconstructions is to look at the reconstructed sea level over the altimetry period and check that the reconstructed spatial trend patterns and variability are similar to the observed one by the altimetry. Fig. 2 shows the spatial trend maps (uniform trend removed) over 1993–2000 (because the C&G reconstruction ends in December 2000) of the altimetry-based reconstruction (Fig. 2a), the C&G reconstruction (see Fig. 2b) and from the two ROM-based reconstructions (Fig. 2c and d). For this comparison, the C&G reconstruction was a posteriori corrected for the IB effect. This was done by simply removing at each time step, NCEP IB grids to the C&G reconstructed sea level.

We note a good agreement between the spatial trend patterns of the reconstructed maps and satellite altimetry presented in Fig. 1a. Our altimetry reconstruction and the C&G reconstruction are very close to each other and they are very consistent with the satellite altimetry signal (Fig. 1a) as expected. The only difference that can be noticed is the lower negative pattern in the Ionian Sea in our altimetry reconstruction. To a lesser extent, the two ROM-based reconstructed trend patterns are consistent as well with the satellite altimetry patterns in each basin but they show a lower negative pattern in the Ionian Sea and a lower positive pattern in the Aegean Sea.

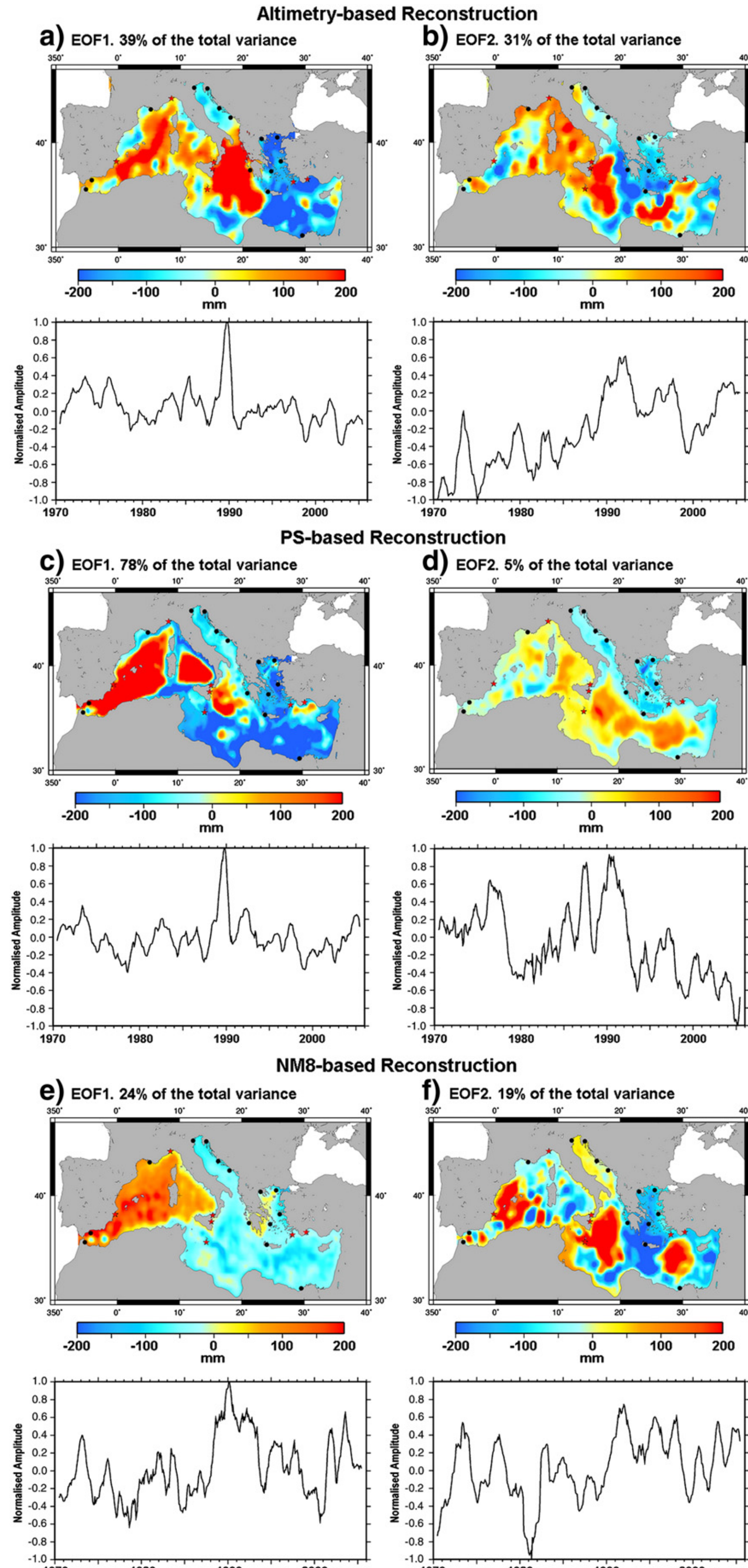

Fig. 5. EOF decomposition over 1970–2006 of the reconstructions. a) and b) show the modes 1 and 2 of the altimetry-based reconstruction. c) and d) show the modes 1 and 2 of the PS-based reconstruction and e) and f) show the modes 1 and 2 of the NM8-based reconstruction. The temporal curves have been smoothed with a 12-month running mean.

We compare as well the reconstructed sea level variability with the observed one over the same period 1993–2000. To do so, we computed, at each grid point, the correlation between the reconstructed time series and the observed altimetry time series over the period 1993–2000. The results are presented in Fig. 3. All reconstructions present positive significant correlations in the central and eastern Mediterranean basins. Correlations are less good in the western basin. C&G reconstruction (Fig. 3b) shows particularly good correlations in the Ionian basin while our altimetry-based reconstruction (Fig. 3a) performs less in this region. This is probably due to the fact that C&G used the tide gage of Valletta over 1989–2000 to do their reconstruction: it must have constrained better their reconstructed variability in this region. Nevertheless our altimetry-based reconstruction seems to perform slightly better in the western basin. It is probably linked to the choice of the tide gages in this region as well. The reconstruction that performs the best in terms of reproduced variability over 1993–2000 appears to be the NM8-based reconstruction (Fig. 3d). The geographically averaged correlations for each case amount to 0.46 for our altimetry based reconstruction, 0.49 for the C&G reconstruction, 0.44 for the PS-based reconstruction and 0.50 for the NM8-based reconstruction. This clearly shows the ability of the model-based reconstructions (especially the NM8-based reconstruction) to reproduce reliably the past sea level variability.

4.2. Validation with tide gage records

Another way to validate the reconstructions over the whole period 1970–2006 is to compare the reconstructed sea level fields with tide gage records that were not taken into account in the reconstruction process.

Note that the coastal tide gage records we use are monthly averages and contain potential contributions from regional or local coastal processes (e.g. local variability of narrow shelf currents, flooding events, wind-forced coastal waves, etc.) as well as land motion unrelated to the signal we are attempting to reconstruct here. Moreover, with the reconstructed sea level fields, the optimal interpolation method uses only part of the total sea level grids variance to reconstruct the total sea level. Consequently, we expect to reconstruct only part of the total observed variance of the tide gage records but it should be representative of the reconstruction validity.

Fig. 4 shows the comparison of the reconstructed fields with 7 tide gage records that were not used in our reconstruction. These are the Alicante and Genova records in the western basin (data from the PSMSL database), the Valletta, Catania and Messina records in the Ionian Sea (data from the Italian tide gage network (www.idromare.it)) and the Rodhos and the Antalya II records in the eastern basin (data from PSMSL). Location of the tide gages is indicated in Fig. 1 (black stars). For each record, we applied the same corrections as explained earlier in Section 2.1: the annual and semi annual signals were removed, and IB and GIA corrections were applied. In Fig. 4, observed tide gage records are plotted in red and reconstructions at the gages location are in black. Table 1 sum up the correlation and the trend differences computed on the basis of this figure. Fig. 4 and Table 1 illustrate the strengths and weaknesses of each of the reconstructions (and of the tide gage records as well):

- In the western Mediterranean, 2 long RLR records from PSMSL, Alicante and Genova, are available to check the reconstructions. Their variability is fairly well reproduced (correlation ~0.5) by both altimetry reconstructions (C&G reconstruction and our reconstruction) (Fig. 4a and b and Table 1 columns 2 and 4). Alicante record variability is exceptionally well reproduced (correlation of 0.67) by the C&G reconstruction certainly because this record is used in their reconstruction process. The trends appear consistent with each other except at Genova for the C&G reconstruction that underestimates its trend by 1.8 mm/yr. Looking at the ROM and our altimetry reconstruction over the whole period (until 2006) (Fig. 4b, c and d and Table 1 columns 5, 9 and 13) the NM8 reconstruction appears to perform better in term of interannual variability.
- The variability at Antalya II is quite well reproduced by both altimetry reconstructions with a similar correlation of ~0.45 (Fig. 4a and b and Table 1 columns 2 and 4) but the C&G reconstruction shows a significantly lower correlation for the Rodhos record (correlation of 0.39) than ours (correlation of 0.57). The model reconstructions (Fig. 4c and d and Table 1 columns 9 and 13) appear homogenous over the Levantine basin with correlations of ~0.5 with both tide gage records (as for the altimetry reconstruction) (Fig. 4a and Table 1 column 5).
- In the Ionian basin, unfortunately we could not find long records to check the reconstructions. The longest available record is the RLR record of Valletta from PSMSL over 1989–2006. Two additional records could be found in the Ionian basin, the Catania and Messina record from the Idromare database (www.idromare.it). These are actually too short to give a reliable verification of the reconstructed trend but they give interesting insights on the interannual variability of the Ionian sea level. The Messina record was selected because of its interesting location. However, it should be taken with caution since it shows many suspicious jumps (in particular in 1998) as previously noticed by Fenoglio-Marc et al. (2004). The two altimetry reconstructions (Fig. 4a and b and Table 1 columns 2 and 4) show very similar correlations with the tide gage records except for the Valletta record that shows higher correlation with the C&G reconstruction (probably because this record was used in the C&G reconstruction). Over 1970–2006, the model reconstructions show consistent, and higher correlations at all tide gages in the Ionian basin than the altimetry reconstruction (Fig. 4a, c and d and column 5, 9 and 13 of Table 1). They show an exceptionally high correlation of 0.68 with the Catania record. As for the trend of the Valletta record it is actually well resolved only by the ROM reconstructions while it is strongly underestimated by the altimetry reconstruction (column 6, 10 and 14 of Table 1).

4.3. Mediterranean sea level variability

In Fig. 5, we present, the 2-D reconstructed fields based on the altimetry dataset, the PS and the NM8 runs respectively. We have performed an EOF decomposition over the whole reconstructed time span 1970–2006 for the three fields. Only the first 2 modes (EOF1 and EOF2) are presented because they account for the largest percentage of the total variance of the signal. The temporal curves have been smoothed with a 12-month running mean in order to emphasize the interannual variability. EOF modes 1 of each of the three reconstructions (Fig. 5a, c and e) – 39, 78 and 24% of total variance respectively – show no trend and a maximum in 1990 in its temporal amplitude. EOF modes 2 (31, 5 and 19% of total variance respectively, see Fig. 5b, d and f) exhibit high and low frequency signal (period ~15 years) over 1970–2006. The EOF spatial patterns differ from one reconstruction to another. We note strong similarities between EOF mode 1 patterns of each reconstruction, with a global dipole marked by a positive pattern in the Western basin and a negative pattern in the Levantine basin. Nevertheless they differ in the Ionian Sea: the NM8 reconstruction shows a negative pattern whereas the altimetry reconstruction shows a positive one and the PS reconstruction a pattern somehow between the both. Concerning the EOF mode 2 patterns, the three reconstructions are fairly consistent in the Ionian and Levantine basin with a strong positive anomaly in the Ionian and Levantine Sea and negative one in the Agean Sea. In the western basin, the altimetry-based and the PS-based reconstructions agree well, with a dipole positive in the eastern part while the NM8-based reconstruction patterns are inversed there. In Fig. 6, the reconstructed basin-average sea level (i.e., the EOF0 of each reconstruction) is shown and compared to the satellite altimetry sea level over 1993–2006. As for the EOFs, it has been smoothed by a 12-month running mean to emphasize the interannual to decadal variability. The four reconstructed sea level curves show the same decadal variability.

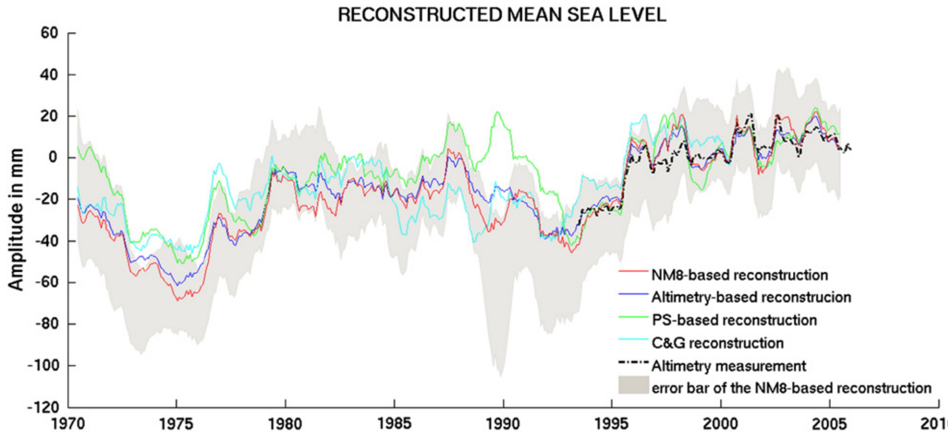

Fig. 6. Basin-average sea level from Satellite altimetry (black dashed line), our altimetry-based reconstruction (blue plain line), the C&G reconstruction (cyan plain line), the PS-based reconstruction (green plain line) and the NM8-based reconstruction (red plain line). The temporal curves have been smoothed with a 12-month running mean.

Their interannual variability is very similar as well over the periods 1970–1985 and 1994–2006. But some differences appear between 1985 and 1995: the PS-based reconstructed basin average sea level shows a high level that does not appear in the other reconstructions. Over the altimetry era, all reconstructions show a mean sea level similar to the observed, altimetry-based global mean sea level. In Fig.6, the gray zone represents the uncertainty in the NM8-based reconstructed mean sea level. This uncertainty is based on the sum of errors due to the least-squares inversion (as presented in Section 3) and errors of the in situ records. This latter error is estimated from a bootstrap method (Efron and Tibshirani, 1993) for standard errors of the in situ water levels for each month (significant at the 95% level).

5. Discussion

The altimetry-based reconstruction developed in this study has been compared with the C&G one over the period 1970–2000 only, because the C&G reconstruction stops in December 2000. We note very similar correlations between the two altimetry-based reconstructions and the tide gage records (Table 1, columns 1 and 3). It suggests that the two altimetry reconstructions are consistent and that the techniques used in C&G and the present study, end up with very close results. This means that removing IB before the reconstruction (this study) or after has little impact on the results.

The Valletta record cannot actually be considered as an independent reference to compare with the two altimetry reconstructions since it is used in C&G reconstruction (between 1995 and 2000) and not in the other (by using only tide gage records that spanned the whole period 1970–2006 and excluding others like Valletta, we ensured the reconstruction to be homogenous over the whole time span). As for the Rhodos record it is not clear why it shows higher correlation with our altimetry reconstruction. An explanation could be that our reconstruction is more constrained in the Levantine basin thanks to the use of the Alexandria record. But this remains to be confirmed.

Considering the reconstructed variability of the basin-averaged Mediterranean sea level, the consistency of the two altimetry reconstructions, while the tide gage dataset differ, gives confidence in the robustness of the results presented by C&G and in this study. However, the spatial trend maps do not match as well (see Fig. 7). The two methods lead to the same basin-averaged trend of ~1.1 mm/yr over 1970–2000 (1.0 mm/yr and 1.2 mm/yr for C&G and this study respectively) but differ in the trend patterns. The two reconstructions show the same geometry in the trend patterns (positive pattern in the Ionian Sea and in the Tyrrhenian Sea) but the C&G reconstruction exhibits lower variability. The comparison of the reconstructions with independent long tide gage record (Table 1) tend to show that in the western basin the trends of our altimetry-based reconstruction are closer to the trends observed at tide gages (see columns 3 and 6 of Table 1 for the Alicante and the Genova records). In the eastern basin, the C&G reconstruction tend to overestimate the trends by ~1 mm/yr while our altimetry reconstruction tend to underestimate the trend at Antalya, as shown by the comparison with the Antalya and the Rodhos tide gage trends. In the Ionian basin the tide gage trends used for the validation are not reliable because of too short records. Both reconstructions seem to underestimate the trend at Valletta, but we cannot extrapolate for the rest of the Ionian Sea.

The three reconstructions presented here (altimetry and ROM based) have been computed by the same process (same tide gage dataset). They only differ by the initial sea level grids used to estimate the spatial variability statistics of the Mediterranean sea level. Looking at the correlations (Table 1, columns 5, 9 and 13) we note a good consistency of the three reconstructed sea level fields: the correlations of each reconstruction with independent tide gages never differ by more than 0.2 from one another. Looking more carefully, both model reconstructions appear particularly consistent since their correlations with tide gages do not differ by more than 0.06, except for the Genova record which has a surprising very low correlation with the PS reconstruction. Hence the two models give similar reconstructed interannual variability. This point gives confidence in the robustness of the model-based reconstruction process. Among the three reconstructions, even if they show similar results, the NM8 reconstruction shows the highest correlations with the test tide gages.

At sub-basin scale, the conclusion is less clear. Some discrepancies appear among the reconstructions. While in the eastern basin, the three reconstructions have similar correlations with the test tide gages, in the western basin, the NM8 and the altimetry reconstruction show higher correlation (see columns 5, 9 and 13 of Table 1 for the Antalya and Rodhos records).

It is in the Ionian Sea where the highest discrepancies can be seen: both model reconstructions show significant higher correlation with the test tide gages of Valletta, Catania and Messina than the altimetry reconstruction. As said earlier, the Ionian basin waters have been strongly impacted by the EMT. This event impacted the Mediterranean circulation during the 1990s until now (Roether et al., 2007) and seems to be responsible for a change in surface circulation, from anti-cyclonic to cyclonic in the Ionian basin in 1998 (Vera et al., 2009). This change in circulation is characterized by the very strong negative pattern in the Ionian Sea that can be seen in the trend maps of the models and the altimetry over the period 1993–2000 (see Fig. 2) (Vera et al., 2009). This exceptional signal dominates the altimetry EOFs since the altimetry dataset only cover the EMT-period (i.e. since 1993). It is less strong in both model-based reconstructions because they capture a long term

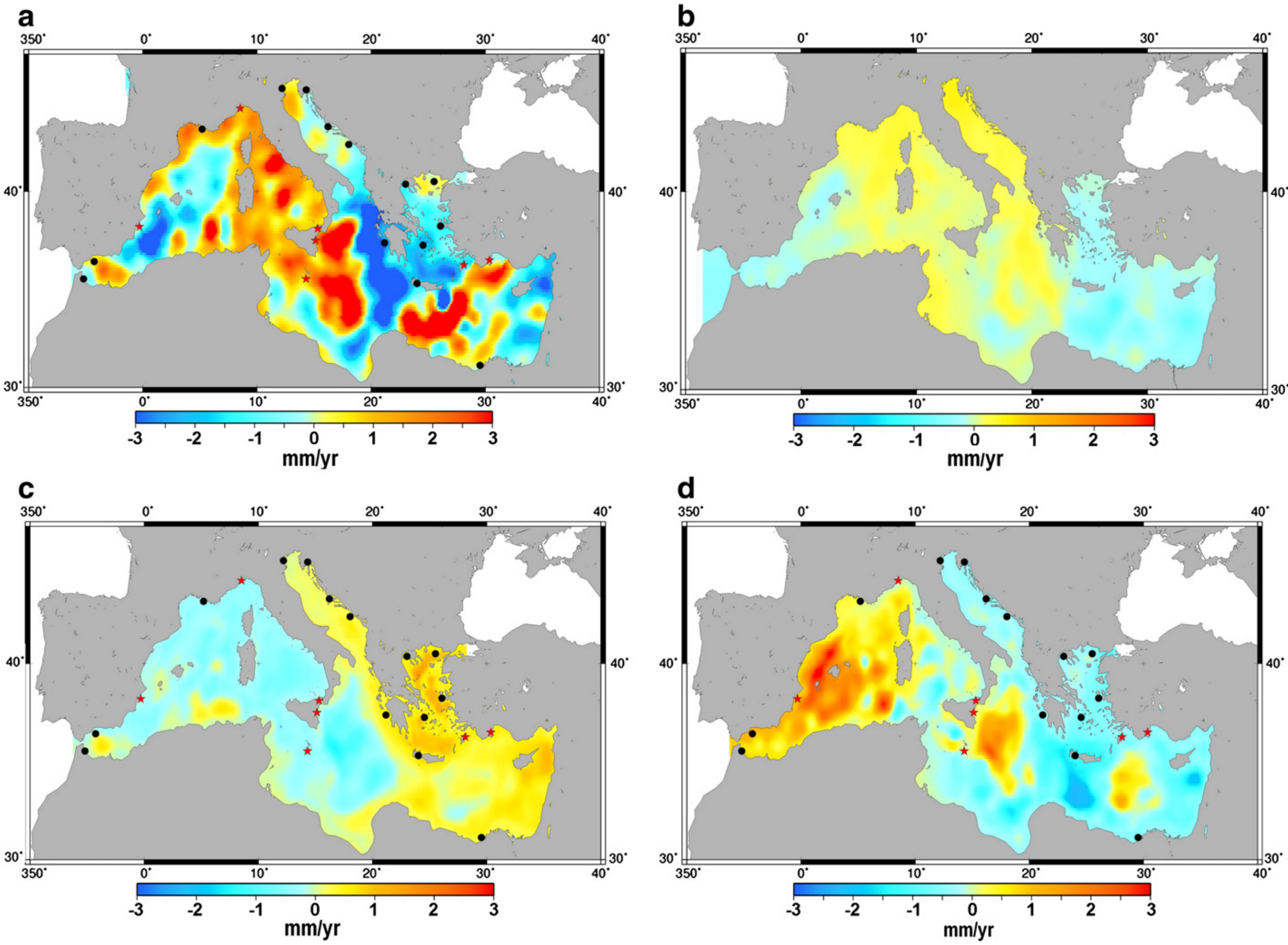

Fig. 7. Map of sea level trends over 1970–2006 of a) the altimetry reconstruction., b) the C&G reconstruction, c) the PS reconstruction and d) the NM8 reconstruction. For each map we have removed the basin-averaged sea level trend computed over 1970–2006 which is of 1.2 mm/yr for the altimetry reconstruction, 1.0 for the C&G reconstruction, 0.8 mm/yr for the PS reconstruction and 1.4 mm/yr for the NM8 reconstruction.

signal not dominated by the EMT event. This could explain the difference of correlations between the reconstructions in the Ionian basin. Looking at Fig. 4a, c and d, the model-based reconstructions appear indeed to better reconstruct the signal prior to the 1990s for the Valletta record for example.

In terms of trends over the period 1970–2000, the three reconstructions of this study plus C&G present strong discrepancies. Only the ROM reconstructions appear to properly reconstruct the Valletta record trend (Table 1 column 15). In the western basin the altimetry-based reconstruction (of this study) is the only one that seems to reproduce both the Genova and Alicante trends. In the eastern basin the trends of Rodhos and Antalya II are not captured by any reconstruction despite their proximity. This point highlights the sensitivity of this region.

The NM8 reconstruction shows better interannual to decadal reconstructed variability so it was used as the reference reconstruction to investigate the potential past influence of some forcing modes of the coupled Atmosphere–Ocean system on the Mediterranean sea level. Fig. 8 compares the amplitude of EOF1 and of the negative EOF2 of the NM8 reconstruction with the North Atlantic Oscillation – NAO – index. For the NAO index we used the monthly index from the Climate Analysis Section NCAR at Boulder, USA (Hurrell, 1995) based on the difference of normalized sea level pressure between Ponta Delgada (Azores) and Reykjavik (Iceland). The NAO index was smoothed by a 12-month running mean and compared to the EOFs of the NM8 reconstruction (smoothed as well by the 12-month running mean). It turns out that before ~1993.5 (date indicated by a gray bar in Fig. 8), the EOF1 temporal curve of the NM8 reconstruction shows a correlation with the NAO index of up to 0.60 (with a significance level >0.99) while over the period 1993.5–2006 the correlation gets down to −0.37. On the other hand, after ~1993.5 the negative EOF2 temporal curve of the NM8 reconstruction shows a high correlation with NAO index of 0.54 (with a SL >0.99) while over the period 1970–1993.5 it only amounts to −0.30. It is interesting to note that the correlation with NAO switches from EOF1 to EOF2 at the epoch of the EMT occurrence.

6. Conclusions

Concerning the interannual/decadal variability of the Mediterranean sea level, the overall agreement of the reconstructions with each other and with the test tide gage records gives confidence in the reconstructed sea level fields. The comparison of model-based reconstructions and altimetry-based reconstructions confirms this robustness since they agree on global scale. At sub-basin scale, the ROM-based reconstructions (especially the NM8-based reconstruction) perform better in the Ionian basin than altimetry-based, and this is probably due to a too strong representation of the EMT event in the altimetry EOFs. This point highlights the advantage of using long ROM

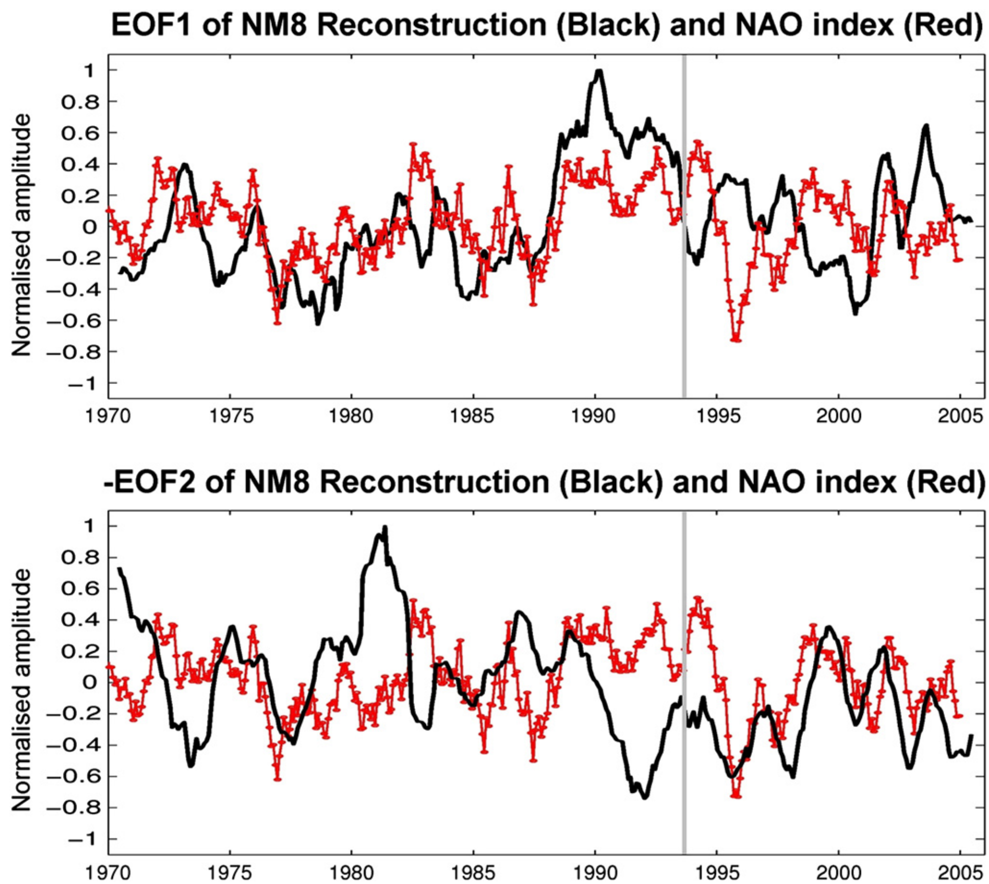

Fig. 8. Comparison of the amplitudes of the NM8 reconstruction EOFs with the NAO index. Top: Amplitude of EOF1 in black and NAO index in red. Bottom: Inverse of the amplitude of EOF2 in black and NAO index in red. The gray line indicates the date 1993.5. The temporal curves have been smoothed with a 12-month running mean.

runs for reconstructing sea level as they capture long-term ocean spatial structure and better reconstruct past sea level.

In term of trends over 1970–2000, no agreement was found between the different reconstructions: the reconstructed fields show trends that differ from the long tide gage record trends by up to 2 mm/yr. The main reason of this difference is probably linked to the Mediterranean sea level interannual to multidecadal variability (of more than 100 mm from one year to the next see Fig. 4). Thus the records are too short to precisely estimate trends. Nevertheless the results suggest that the ROM-based reconstructions give the better trend estimate in the Ionian Sea while the altimetry reconstructions seem to be closer to real trends in the western basin. To sum up, the NM8-based reconstruction shows the highest correlation with test tide gages. The mean sea level trend reproduced by the NM8 reconstruction is of 1.4 mm/yr (over 1970–2000).

Gomis et al. (2008) and Marcos and Tsimplis (2008) >showed that the NAO drove the atmospheric-induced (wind stress + atmospheric pressure) sea level variability in the Mediterranean basin between 1960 and 1990. Here the comparison of the NM8 reconstruction EOFs with the NAO index suggests that between 1970 and the beginning of the 1990s, NAO forcing strongly impacts as well the IB-corrected Mediterranean sea level variability. But since then, NAO forcing has modified its impact on the sea level spatial patterns. The strong impact of the basin-scale water mass redistribution after the EMT event that lasted at least a decade probably plays some role (Herrmann et al., 2010). This redistribution could have had an impact on the steric component (East–west gradient) and on the circulation component (Ionian Sea) at decadal time scale. But the mechanism for this needs further investigation. In particular, further study using sensitivity runs with regional ocean models has to be done to better attribute the Mediterranean sea level variability in the 90s.

Acknowledgments

We would like to thank our colleague O. Frihy of the Coastal Research Institute at Alexandria for kindly providing us with the Alexandria tide gage record and S. Zerbini for providing us with the tide gage records of the idromare dataset. We would like to thank as well Florence Sevault (Météo-France, CNRM-GAME) for developing, maintaining and running the NEMOMED8 regional ocean model. A special thank to Volfango Rupolo who contributed to this work with his enthusiasm for science and with his happiness. Unfortunately, it has been our last chance to collaborate with him on this earth as he passed away on April 2010.

Finally we are very grateful to L. Fenoglio-Marc for her thorough review and to an anonymous reviewer for his/her useful comments.

We would like to acknowledge the support and financial contribution of the Topo-Europe programme and CECILE programme.

References

Ablain, M., Cazenave, A., Valladeau, G., Guinehut, S., 2009. A new assessment of the error budget of global mean sea level rate estimated by satellite altimetry over 1993–2008. Ocean Sci. 5, 193–201.

Artale, V., Calmanti, S., Carillo, A., Dell'Aquila, A., Herrmann, M., Pisacane, G., Ruti, P.M., Sannino, G., Struglia, M.V., 2009. An atmosphere–ocean regional climate model for

the Mediterranean area: assessment of a present climate simulation. Ocean Modelling 30, 56–72.
Becker, M., Karpytchev, M., Davy, M., Doekes, K., 2009. Impact of a shift in mean on the sea level rise: application to the tide gauges in the Southern Netherlands. Continental Shelf Res. 29, 741–749.
Beuvier, J., Sevault, F., Herrmann, M., Kontoyiannis, H., Ludwig, W., Rixen, M., Stanev, E., Beranger, K., Somot, S., 2010. Modelling the Mediterranean Sea interannual variability during 1961–2000: focus on the Eastern Mediterranean Transient (EMT). J. Geophys Res. 115, C08017. doi:10.1029/2009JC005850.
Bindoff, N.L., Willebrand, J., Artale, V., Cazenave, A., Gregory, J.M., Gulev, S., Hanawa, K., Le Quéré, C., Levitus, S., Nojiri, Y., Shum, C.K., Talley, L.D., Unnikrishnan, A.S., 2007. Observations: oceanic climate change and sea level. Climate Change 2007: The Physical Science Basis. Cambridge University Press, pp. 385–432.
Cabanes, C., Cazenave, A., Le Provost, C., 2001. Sea level change from Topex-Poseidon altimetry for 1993–999 and possible warming of the southern oceans. Geophys. Res. Lett. 28, 9–12.
Calafat, F.M., Gomis, D., 2009. Reconstruction of Mediterranean sea level fields for the period 1945–2000. Glob. Planet. Change 66, 225–234.
Carrere, L., Lyard, F., 2003. Modeling the barotropic response of the global ocean to atmospheric wind and pressure forcing — comparisons with observations. Geophys. Res. Lett. 6, 1275. doi:10.1029/2002GL016473.
Church, J.A., White, N.J., Coleman, R., Lambeck, K., Mitrovica, J.X., 2004. Estimates of the regional distribution of sea level rise over the 1950–2000 period. J. Clim. 17, 2609–2625.
Déqué, M., Piedelievre, J.P., 1995. High-resolution climate simulation over Europe. Clim. Dyn. 11, 321–339.
Efron, B., Tibshirani, R.J., 1993. An Introduction to the Bootstrap. Chapman & Hall.
Fenoglio-Marc, L., Groten, E., Dietz, C., 2004. Vertical land motion in the Mediterranean sea from altimetry and tide gauge stations. Marine Geodey 27, 683–701.
Frihy, O.E., Deabes, E.A., Shereet, S.M., Abdalla, F.A., 2010. Alexandria-Nile Delta coast, Egypt: update and future projection of relative sea-level rise. Earth Environment Science 2, 253–273. doi:10.1007/s12665-009-0340-x.
Gomis, D., Ruiz, S., Sotillo, M.G., Alvarez-Fanjul, E., Terradas, J., 2008. Low frequency Mediterranean sea level variability: the contribution of atmospheric pressure and wind. Glob. Planet. Change 63, 215–229.
Greatbatch, R.J., 1994. A note on the representation of steric sea-level in models that conserve volume rather than mass. J. Geophys. Res. 99, 12767–12771.
Herrmann, M.J., Somot, S., 2008. Relevance of ERA40 dynamical downscaling for modeling deep convection in the Mediterranean Sea. Geophys. Res. Lett. 35, L04607. doi:10.1029/2007GL032442.
Herrmann, M., Sevault, F., Beuvier, J., Somot, S., 2010. What induced the exceptional 2005 convection event in the northwestern Mediterranean basin? Answers from a modeling study. J. Geophys. Res. 115, C12051. doi:10.1029/2010JC006162.
Hurrell, J.W., 1995. Decadal trends in the North Atlantic Oscillation — regional temperatures and precipitations. Science 269, 676–679.
Josey, S.A., 2003. Changes in the heat and freshwater forcing of the eastern Mediterranean and their influence on deep water formation. J. Geophys. Res. 108, 3237–3255. doi:10.1029/2003JC001778.
Kalnay, E., Kanamitsu, M., Kistler, R., Collins, W., Deaven, D., Gandin, L., Iredell, M., Saha, S., White, G., Woollen, J., Zhu, Y., Chelliah, M., Ebisuzaki, W., Higgins, W., Janowiak, J., Mo, K.C., Ropelewski, C., Wang, J., Leetmaa, A., Reynolds, R., Jenne, R., Joseph, D., 1996. The NCEP/NCAR 40-year reanalysis project. Bull. Amer. Meteor. Soc. 77, 437–471.
Kaplan, A., Kushnir, Y., Cane, M.A., 2000. Reduced space optimal interpolation of historical marine sea level pressure: 1854–1992. J. Clim. 13, 2987–3002.
Klein, B., Roether, W., Manca, B.B., Bregant, D., Beitzel, V., Kovacevic, V., Luchetta, A., 1999. The large deep water transient in the Eastern Mediterranean. Deep Sea Res. I. 46, 371–414.
Lascaratos, A., Roether, W., Nittis, K., Klein, B., 1999. Recent changes in deep water formation and spreading in the eastern Mediterranean Sea: a review. Progress in Oceanography 44, 5–36.
Le Traon, P.Y., Nadal, F., Ducet, N., 1998. An improved mapping method of multisatellite altimeter data. J. atmospheric oceanic technology 15, 522–534.
Le Traon, P.Y., Ogor, F., 1998. ERS-1/2 orbit improvement using TOPEX/POSEIDON: the 2 cm challenge. J. Geophys. Res. 103, 8045–8057.
Llovel, W., Cazenave, A., Rogel, P., Lombard, A., Nguyen, M.B., 2009. Two-dimensional reconstruction of past sea level (1950–2003) from tide gauge data and an Ocean General Circulation Model. Climate of the Past 5, 217–227.
Lombard, A., Cazenave, A., DoMinh, K., Cabanes, C., Nerem, R.S., 2005. Thermosteric sea level rise for the past 50 years; comparison with tide gauges and inference on water mass contribution. Glob. Planet. Change 4, 303–312.
Madec, G., 2008. Nemo ocean engine. Note du pôle modélisation no. 27. IPSL France. ISSN n°1288–1619.
Malanotte-Rizzoli, P., Manca, B.B., d'Alcala, M.R., Theocharis, A., Brenner, S., Budillon, G., Ozsoy, E., 1999. The Eastern Mediterranean in the 80s and in the 90s: the big transition in the intermediate and deep circulations. Dynamics of Atmospheres and Oceans 29, 365–395.
Marcos, M., Tsimplis, M.N., 2007. Variations of the seasonal sea level cycle in southern Europe. J. Geophys. Res. 112, C12011. doi:10.1029/2006JC004049.
Marcos, M., Tsimplis, M.N., 2008. Coastal sea level trends in southern Europe. Int. J. Geophys. 175, 70–82.
Milne, G.A., Gehrels, W.R., Hughes, C.W., Tamisiea, M.E., 2009. Identifying the causes of sea-level change. Nature Geoscience 2, 471–478.
Pal, J.S., Giorgi, F., Bi, X.Q., Elguindi, N., Solmon, F., Gao, X.J., Rauscher, S.A., Francisco, R., Zakey, A., Winter, J., Ashfaq, M., Syed, F.S., Bell, J.L., Diffenbaugh, N.S., Karmacharya, J., Konare, A., Martinez, D., da Rocha, R.P., Sloan, L.C., Steiner, A.L., 2007. Regional climate modeling for the developing world — the ICTP RegCM3 and RegCNET. Bull. Amer. Meteor. Soc. 88, 1395–1409.
Peltier, W.R., 2004. Global glacial isostasy and the surface of the ice-age earth: the ice-5G (VM2) model and grace. Ann. Rev. Earth Planet. Sci. 32, 111–149.
Preisendorfer, R.W., 1988. Principal component analysis in meteorology and oceanography. Developments in Atmospheric Science, vol. 17. Elsevier. 425 pp.
Rixen, M., Beckers, J.M., Levitus, S., Antonov, J., Boyer, T., Maillard, C., Fichaut, M., Balopoulos, E., Iona, S., Dooley, H., Garcia, M.J., Manca, B., Giorgetti, A., Manzella, G., Mikhailov, N., Pinardi, N., Zavatarelli, M., 2005. The western Mediterranean deep water: a proxy for climate change. Geophys. Res. Lett. 32, L12608. doi:10.1029/2005GL022702.
Roether, W., Manca, B.B., Klein, B., Bregant, D., Georgopoulos, D., Beitzel, V., Kovacevic, V., Luchetta, A., 1996. Recent changes in eastern Mediterranean deep waters. Science 271, 333–335.
Roether, W., Klein, B., Manca, B.B., Theocharis, A., Kioroglou, S., 2007. Transient Eastern Mediterranean deep waters in response to the massive dense-water output of the Aegean Sea in the 1990s. Progress in Oceanography 74, 540–571.
Roullet, G., Madec, G., 2000. Salt conservation, free surface, and varying levels: a new formulation for ocean general circulation models. J. Geophys. Res. 105, 23927–23942.
Samuel, S., Haines, K., Josey, S., Myers, P.G., 1999. Response of the Mediterranean Sea thermohaline circulation to observed changes in the winter wind stress field in the period 1980–1993. J. Geophys. Res. 104, 7771–7784.
Sevault, F., Somot, S., Beuvier, J., 2009. A regional version of the NEMO ocean engine on the Mediterranean sea: NEMOMED8 user's guide. Note de centre no 107, CNRM, Toulouse, France.
Steigenberger, P., Rothacher, M., Dietrich, R., Fritsche, M., Rulke, A., Vey, S., 2006. Reprocessing of a global GPS network. J. Geophys. Res. 111, B05402. doi:10.1029/2005JB003747.
Stocchi, P., Spada, G., 2009. Influence of glacial isostatic adjustment upon current sea level variations in the Mediterranean. Tectonophysics 474, 56–68.
Struglia, M.V., Mariotti, A., Filograsso, A., 2004. River discharge into the Mediterranean Sea: climatology and aspects of the observed variability. J. Clim. 17, 4740–4751.
Theocharis, A., Nittis, K., Kontoyiannis, K., Papageorgiou, E., Balopoulos, E., 1999. Climatic changes in the Aegean Sea influence the Eastern Mediterranean thermohaline circulation (1986–1997). Geophys. Res. Lett. 26, 1617–1620.
Theocharis., A., Kontoyiannis, K., 1999. Interannual variability of the circulation and hydrography in the Eastern Mediterranean (1986–1995). In: Kluwer Academic Publishing (Ed) NATO Sciences Series. Dordrecht, The Netherlands pp453–464.
Toumazou, V., Cretaux, J.F., 2001. Using a Lanczos eigensolver in the computation of empirical orthogonal functions. Mon. Weather Rev. 129, 1243–1250.
Tsimplis, M.N., Josey, S., 2001. Forcing of the Mediterranean Sea by atmospheric oscillations over the North Atlantic. Geophys. Res. Lett. 28, 803–806.
Tsimplis, M.N., Alvarez-Fanjul, E., Gomis, D., Fenoglio-Marc, L., Perez, B., 2005. Mediterranean Sea level trends: atmospheric pressure and wind contribution. Geophys. Res. Lett. 20, L20602. doi:10.1029/2005GL023867.
Tsimplis, M.N., Marcos, M., Colin, J., Somot, S., Pascual, A., Shaw, A.G.P., 2009. Sea level variability in the Mediterranean Sea during the 1990s on the basis to two 2d and one 3d model. J. Marine Systems. 18, 109–123. doi:10.1016/j.jmarsys.2009.04.003.
Uppala, S.M., Kallberg, P.W., Simmons, A.J., Andrae, U., Bechtold, V.D., Fiorino, M., Gibson, J.K., Haseler, J., Hernandez, A., Kelly, G.A., Li, X., Onogi, K., Saarinen, S., Sokka, N., Allan, R.P., Andersson, E., Arpe, K., Balmaseda, M.A., Beljaars, A.C.M., Van De Berg, L., Bidlot, J., Bormann, N., Caires, S., Chevallier, F., Dethof, A., Dragosavac, M., Fisher, M., Fuentes, M., Hagemann, S., Holm, E., Hoskins, B.J., Isaksen, L., Janssen, P.A.E.M., Jenne, R., McNally, A.P., Mahfouf, J.F., Morcrette, J.J., Rayner, N.A., Saunders, R.W., Simon, P., Sterl, A., Trenberth, K.E., Untch, A., Vasiljevic, D., Viterbo, P., Woollen, J., 2005. The ERA-40 re-analysis. Quarterly J. Royal Meterological Society 131, 2961–3012.
Valcke, S., Redler, R., 2006. OASIS3 user guide. PRISM support Initiative report no 4. 60 pp.
Vera, J.D., Criado-Aldeanueva, F., Garcia-Lafuente, J., Soto-Navarro, F.J., 2009. A new insight on the decreasing sea level trend over the Ionian basin in the last decades. Glob. Planet. Change 68, 232–235.
Volkov, D.L., Larnicol, G., Dorandeu, J., 2007. Improving the quality of satellite altimetry data over continental shelves. J. Geophys. Res. 112, C06020. doi:10.1029/2006JC003765.
Woodworth, P.L., Player, R., 2003. The permanent service for mean sea level: an update to the 21st century. J. Coast. Res. 19, 287–295.
Woppelmann, G., Miguez, B.M., Bouin, M.N., Altamimi, Z., 2007. Geocentric sea-level trend estimates from GPS analyses at relevant tide gauges world-wide. Glob. Planet. Change 57, 396–406.
Woppelmann, G., Letetrel, C., Santamaria, A., Bouin, M.N., Collilieux, X., Altamimi, Z., Williams, S.P.D., Martin Miguez, B., 2009. Rates of sea level change over the past century in a geocentric reference frame. Gephys. Res. Lett. 36, L12607. doi:10.1029/2008GL038720.
Zervakis, V., Georgopoulos, D., Karageorgis, A.P., Theocharis, A., 2004. On the response of the Aegean sea to climatic variability: a review. Int. J. Climat. 24, 1845–1858.